IEEE Access
Multidisciplinary | Rapid Review | Open Access Journal

Received November 11, 2021, accepted December 10, 2021, date of publication December 15, 2021,
date of current version December 27, 2021.

Digital Object Identifier 10.1109/ACCESS.2021.3135883

Impact of Geomagnetically Induced Currents on High Voltage Transformers in Malaysian Power Network and Its Mitigation

Z. M. KHURSHID[1], N. F. AB AZIZ[1], (Member, IEEE), Z. A. RHAZALI[1], AND M. Z. A. AB KADIR[2], (Senior Member, IEEE)

[1]College of Engineering, Universiti Tenaga Nasional, Kajang, Selangor 43000, Malaysia
[2]Advanced Lightning, Power and Energy Research Centre (ALPER), Faculty of Engineering, Universiti Putra Malaysia, Serdang, Selangor 43000, Malaysia

Corresponding author: Z. M. Khurshid (zmnako24@hotmail.com)

This work was supported in part by the Ministry of Higher Education (MOHE) of Malaysia under Grant 20180112FRGS, and in part by the Universiti Tenaga Nasional through UNITEN Bold Grant.

ABSTRACT Geomagnetically induced current (GIC) is a ground end manifestation of geomagnetic disturbances (GMDs) and space weather arising from solar activity, which causes half-cycle saturation and represents a potential hazard for a stable and safe operation of earthed high voltage (HV) power transformers. Previous studies have shown that the impact of GIC is not limited to high and mid-latitude regions, but it can also affect power systems located in lower geographic latitudes. This work presents the impact of GIC on HV transformers in the Malaysian power network. A detailed power network was modelled using the Power System Computer-Aided Design for Electromagnetic Transients including Direct Current (PSCAD/EMTDC) software. The entire network was subjected to a geoelectric field strength of 20 V/km at the northward and eastward directions. The GIC analysis has determined the most critical locations in the power network model that are prone to high GICs. The simulation results demonstrated that the most vulnerable substations to GMD events and experience the most severe GICs were those located in the middle of the Malaysian power network. The GIC effects and saturation levels of four transformers' types in these locations have been investigated over the transmission network. Under the GIC condition, transformers were driven into half-cycle saturation and their reactive power consumption drastically increased. Thus, conventional GIC mitigation systems based on neutral blocking devices (NBDs) were proposed and connected to the power transformers to block the GIC flow in their neutral paths. It was found that the GIC protection modes in the mitigation systems effectively eliminate the injected GICs in the neutral paths and are able to prevent the saturation occurrence of the transformers.

INDEX TERMS Geomagnetically induced current, geomagnetic disturbance, space weather, PSCAD/EMTDC, high voltage transformers, malaysian power network.

I. INTRODUCTION

The Geomagnetically Induced Current (GIC) is a phenomenon that occurs during space weather or Geomagnetic Disturbance (GMD). It is considered one of the most hazardous phenomena associated with space weather and solar activities. These disturbances are masses of electromagnetic fields and particles, known as Coronal Mass Ejections (CMEs) that are emanated by the Sun during solar activity. Sometimes these CMEs are many times larger than the Earth thrown out from the Sun in a specific direction and can travel at speeds about 2000 kilometres per second (km/s) in space [1]–[4]. Note that CMEs are only one kind of driver. There are also corotating interaction regions (CIRs) and interplanetary (IP) shocks that cause GMDs [5]–[9]. Moreover, large GICs in power lines can also be induced by detonating nuclear bombs at an altitude of 30 km above the Earth's surface or higher, commonly known as a High-altitude Nuclear Electro-Magnetic Pulse (HEMP). The gamma particles are spread over a wide area by such detonation and collide with air molecules. These collisions result in ionization of the atmospheric layer and create an electromagnetic signal that

The associate editor coordinating the review of this manuscript and approving it for publication was Michele Magno.

might interact with electrical power networks and lead to GIC [10], [11].

When CMEs strike the magnetic field of the Earth which provides protection against the fast-moving plasma becomes compressed and results in a varying magnetic field on the ground. This magnetic field variation generates a geoelectric field on the Earth's surface and leads to GIC flow through man-made technology [2]–[4], [12]. This GIC exhibits a very low-frequency quasi-Direct Current (DC) (less than 1 Hz) with amplitudes of 10–15 A and up to 300 A peak current for 1–2 minutes that flows along conductors and technological infrastructure [13], [14]. The power transformers which are connected by transmission lines are the most affected by GIC events. The GIC enters from the neutral ground point of the star-connected (wye) transformer windings and divides equally among the phases [15], [16]. When the GIC flows through the transformer windings, a DC magnetic flux is generated in the core, whose magnitude depends on the GIC flow magnitude. This DC flux is then superimposed on the AC flux in such a way that the asymmetrical saturation takes place in the magnetic cores of the transformers (half-cycle saturation) and increases their reactive power consumptions critically.

During saturation phenomenon, transformers draw an extremely large asymmetrical exciting distorted current that is rich in even and odd harmonics [17]–[21]. These harmonics can trigger the relays improperly, overheating the generators and transformer's windings and cores, leading to unstable operations of the power system and could result in long-term damage to the system's components. These effects may turn into catastrophic failures (i.e., permanent damage or blackouts) if they persist for a few minutes. The 1989 geomantic storm in North America [16], [18], [22]–[24] that lead to severe economic losses [2] is an example of such catastrophic consequence due to the effects of GIC. Besides, a review of previous studies has shown that the GMD effects are not limited to power systems in high and mid-latitude countries but also extend to HV power systems at lower geographic latitudes and equatorial regions [25]. Therefore, this research aims to investigate the impacts of GMD on different types of HV power transformers in a power grid in Malaysia that is located a few degrees south of the equatorial electrojet (EEJ) current, an ionospheric current that ''snakes'' around the Earth along the magnetic equator. Previous works showed that IP shocks are the main cause of the EEJ current enhancement because the auroral electrojets are far at high latitudes. Other previous works showed that IP shocks that strike Earth nearly head-on may further compress and enhance EEJ current effects leading to higher geomagnetic perturbations related to GICs if stations and substations are located near the local noon [5], [6], [8], [26]–[32].

A complete system that considers all network parameters and variations is modelled using Power System Computer-Aided Design for Electromagnetic Transients including Direct Current (PSCAD/EMTDC) software. The PSCAD/EMTDC is an industry-standard simulation tool for studying the transient behaviour of electrical networks in the time-domain [33] which is commercially available online [34]. The PSCAD model in this work has been designed to study the GIC effects on the power transformers in the Malaysian power system. In addition, the produced GICs in the system were calculated based on the nodal admittance matrix method (NAMM) due to the given geoelectric field. The correct assessment and mitigation effects of GMD on HV power grids require detailed analysis considering the influence of all factors that may contribute to increasing the GIC risks. In addition, a conventional GIC mitigation system is proposed and tested in PSCAD to block or reduce the related effects. This paper is divided into the following sections. In the second section, the modelling design of the system is presented, which includes the PSCAD modelling design of the power network, the GIC calculation method and the modelling design of the GIC mitigation. In the third section, the results of the simulation cases are presented. Finally, the fourth section presents the conclusion and perspectives of this paper.

II. MODELING OF POWER NETWORK

The Malaysian power network was modelled using PSCAD/EMTDC software to investigate the GIC effects on HV power transformers from different viewpoints and to mitigate the related impact with the application of conventional GIC neutral blocking device (NBD) systems. The PSCAD layout of the power network is illustrated in Fig. 3. The PSCAD library provides users with many function blocks, which help to build and design custom electrical devices and different NBDs according to the system requirements and GIC values.

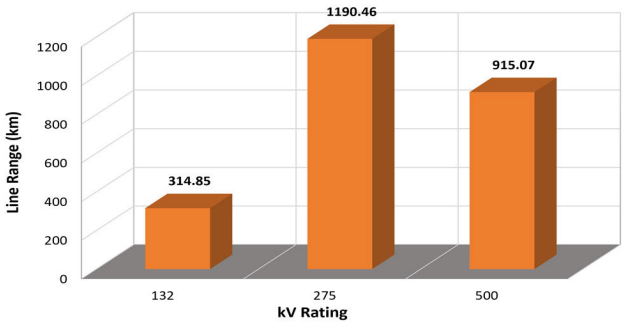

FIGURE 1. Transmission line length with the rated voltage used for the design.

The modelled power network comprises 54 substations, 138 buses which are linked through transmission lines at the voltages of 500 kV, 275 kV, and 132 kV. A total of 117 transformers with different operating voltages was also included in the system (Figs. 1 and 2). The power utility company in Malaysia provided the system's data. Given that GICs are strongly dependent on the grid topology with higher operating voltages of the grid implying smaller conductor resistances, thus, the probability of GIC effects is higher.

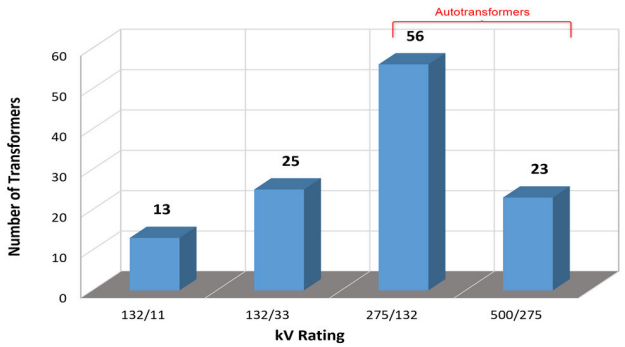

FIGURE 2. Number of transformers with the rated voltage used for the design.

In addition, the grid expansion leads to a strong increase in the intensity of GIC in substations [18]. In general, a modern power system is divided into four major parts: generation, transmission, distribution, and loads [35], and only the first three parts are essential for the GIC modelling analysis [36]. Considering the unity power factor (ideal case), this work only connected pure active loads to the system.

The bus voltages of the system in PSCAD are presented in Fig. 4. According to the voltage regulation requirements in Malaysia at steady-state operating condition [37], all bus voltages were within the permissible limits between 0.95 pu and 1.15 pu.

A. GIC CALCULATION

In this simulation case, the vulnerability of the power network to GICs is performed considering the worst-case geomagnetic storm scenarios by applying the uniform geoelectric field with a value of 20 V/km to the power network model at the northward and eastward directions. This field value was selected to represent a 1 in 100 years storm scenario that could occur during a severe GMD in a certain region, where the Earth's conductivity is low [38], [39]. This analysis will assist in estimating the power grid response under such geoelectric field amplitude, which may occur in the future, as well as to identify the most critical locations that require NBD(s) installation. Also, it helps to test the efficacy of related mitigation systems under a worst-case scenario.

The produced GICs due to the applied geoelectric field are calculated across the Malaysian power network based on NAMM. n the NAMM analysis, a circuit model of the power network is treated as DC with consideration of DC resistance parameters of system components since the GIC has a very low-frequency range from power systems viewpoint. For the GIC calculation, only windings that have physical connections to the ground, such as grounded wye connections are considered since they provide the GIC flow path. Windings without a physical connection to ground and mutual coupling windings, such as ungrounded wye and delta windings are excluded [28]. In [25], a detailed derivation of GIC calculation based on DC analysis was presented.

B. GIC MITIGATION SYSTEM

A GIC mitigation system was modelled in PSCAD software based on a conventional NBD concept presented in [10], [40]. The system consists of three operational modes comprising solid ground, GIC protection, and ground fault protection, as presented in Fig. 5.

The solid ground mode is modelled by an AC breaker and a DC disconnect breaker connected in series through a shunt resistor (0.001 Ω) to the ground. The breakers are built in the PSCAD/EMTDC model with different options. The option "open possible at any current" at the AC ground switch was disabled, and the current chopping limit was set at zero. The DC disconnect switch is modelled and enabled to open at any current. The AC breaker has a HV stand-off used to protect a DC breaker from any overvoltages, and a DC breaker is used to break DC and quasi-DC currents. The GIC protection mode consists of a 50 kW (1 Ω) power resistor connected in series with a capacitor bank to the ground, where the capacitor value (3180 μF) is equal to (1 Ω impedance) at 50 Hz. The capacitance of the capacitor bank for 1 Ω impedance was calculated using the following equations.

$$Xc = \frac{1}{2\pi fC} = 1 \tag{1}$$

$$C = \frac{1}{2\pi fXc} \tag{2}$$

$$C = \frac{1}{2\pi \times 50 \times 1} = 3183\mu F \tag{3}$$

where f is the system frequency equal to 50 Hz, and C is the capacitance of the capacitor bank. A signal from the shunt resistor (0.001 Ω) is used to detect any DC current or GIC. This signal and/or detected induced harmonic from the bus voltages of power transformer due to the GIC is then used to trigger the system into the GIC protection mode and effectively block DC or quasi-DC currents in the neutral path of a transformer. The generated trip signal from the control circuit is used to trigger (open) the AC and DC switches during the GIC events. The flowchart process of the control circuit is depicted in Fig. 6. The fault protection mode is comprised of a 4 kV metal oxide varistor (MOV) surge arrester connected in parallel with the GIC protection mode to protect the capacitor bank and transformer from any overvoltage that might build up across the capacitor during potential ferroresonance conditions from any phase to the ground faults. The parameters of the GIC mitigation system are presented in Table 1.

TABLE 1. Parameters of the GIC mitigation system.

Shunt Resistor	0.001 Ω
Series Resistor	1 Ω
Capacitor Bank	3180 µF
Operating Frequency	50 Hz
MOV Rating	4 kV
MOV Clamping Voltage	3.67 kV
Delay Time of Control System	2 Seconds

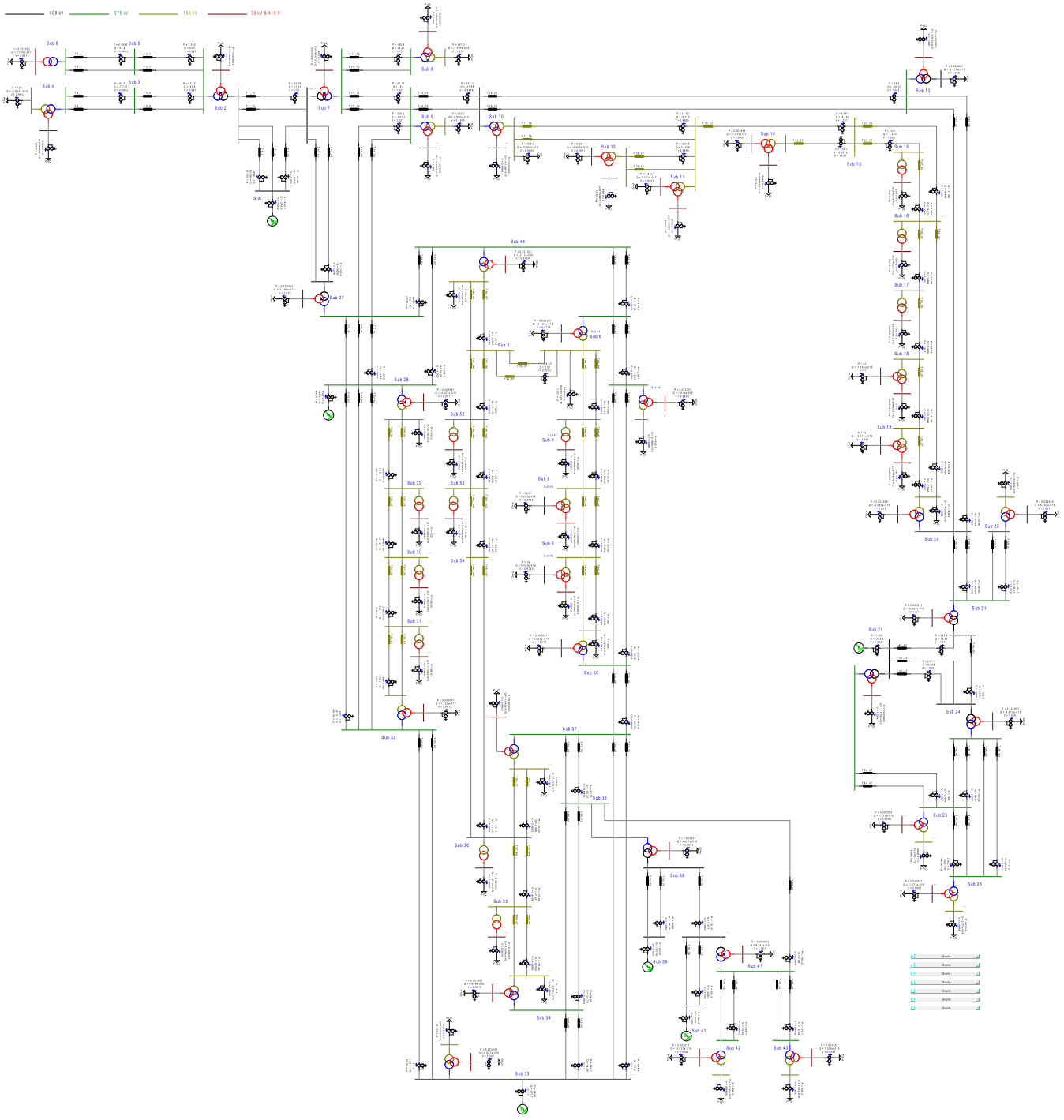

FIGURE 3. PSCAD Modelling design of the system.

III. RESULTS AND DISCUSSION

Three case studies were carried out in this section, including GIC calculation in the power network, the effect of GIC on the transformer operation, and mitigation device operation during the GIC event. The simulation results of these cases are presented and discussed in detail in the following subsections, respectively.

A. SIMULATION RESULTS OF CASE 1

In this simulation case, the produced GICs were calculated in the Malaysian power network model using the NAMM due to the geoelectric field value of 20 V/km which uniformly applied to the entire system at 0° northward and 100° eastward directions. The results of only two directions were presented because these angles are considered the main

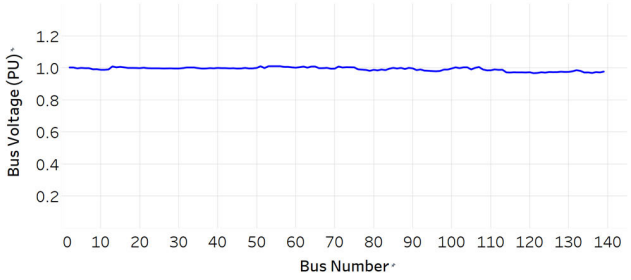

FIGURE 4. Bus voltages of the system in PSCAD.

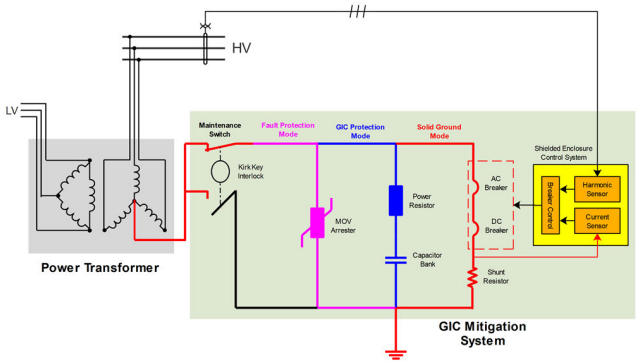

FIGURE 5. GIC mitigation system.

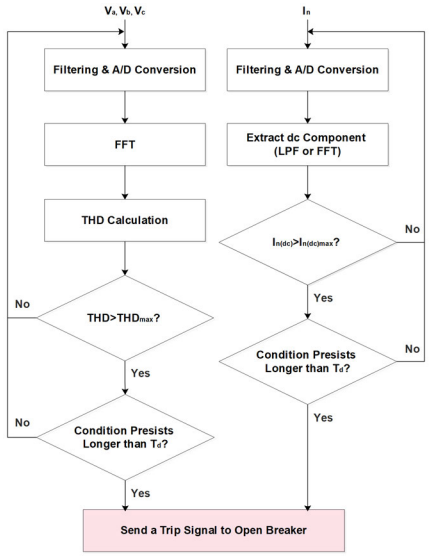

FIGURE 6. Flowchart of the control circuit.

field directions that generate the highest GICs in most cases [41]–[50]. In this work, the 100° field angle contributes the highest GICs in the entire system. The grounding resistance of substations was set at 0.8 Ω. The results of induced currents at the substations are presented in Fig. 7. As seen from Fig. 7(a), the produced GICs across the system at 0° are in the range between +608 A at substation 4 and −630 A at substation 22. The results showed that the GICs tend to remain either positive or negative at a particular site throughout the modelled storms [51]. The behaviour of the GICs in the power network depends on the induced DC current in the power lines and the resistance values of different elements in the system [47].

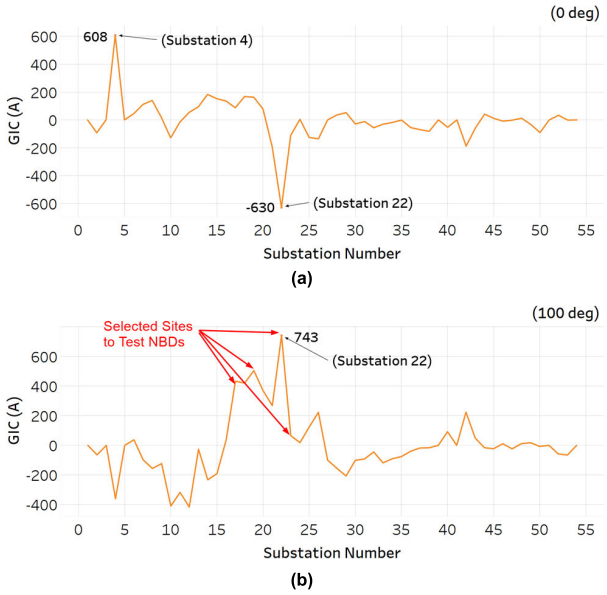

FIGURE 7. The response of the Malaysian power network model to 20 V/km electric field with respect to total GIC flow into substation ground grids at field angle (a) 0° northward direction and (b) 100° eastward direction. Positive GIC (current flowing into the bus) and negative GIC (current flowing into the ground).

When the field angle was changed from 0° to 100° eastward direction, the polarities and values of the GICs across substations also changed. Most of the substations located in the middle of the Malaysian power network experienced higher induced GICs, especially substations (17-22), as shown in Fig. 7(b). Transformers at these locations were the prime candidates to be protected by GIC mitigation systems given that they are the most vulnerable to GMD events as well as the most critical to the stability of the power system since they draw the highest reactive powers during space weather events [52]. The maximum GIC was obtained at substation 22 with a value of 743 A, as depicted in Fig. 7(b). Also, the obtained high GICs in the middle of the system are due to long transmission lines connected to these substations with respect to different voltage levels. The GIC was zero at substations that do not contain the neutral grounded transformers since there is no ground path for the GIC to flow into the system.

The adequacy of the GIC analysis results in this case was validated using the IEEE benchmark test system that was provided by Horton *et al.* [49]. The system was imposed to a 1 V/km geoelectric field in the 0° northward and 90° eastward directions. The results of substation' GIC of the test system were compared with the results based on the NAMM and denoted in blue and red colour, respectively, as depicted in Fig.8. The figure shows that the substations GIC results

TABLE 2. Critical locations that experience high GICs with respect to the different transformers due to geoelectric field 20 V/km.

Type	Rated Voltage (kV)	Rated MVA	Substation No.	GIC (A)
Autotransformer	500/275	1050	21	268
Autotransformer	275/132	180	22	743
Standard Transformer	132/33	45	17	433
Standard Transformer	132/11	30	19	505

were extremely close for both the northward and eastward geoelectric field directions.

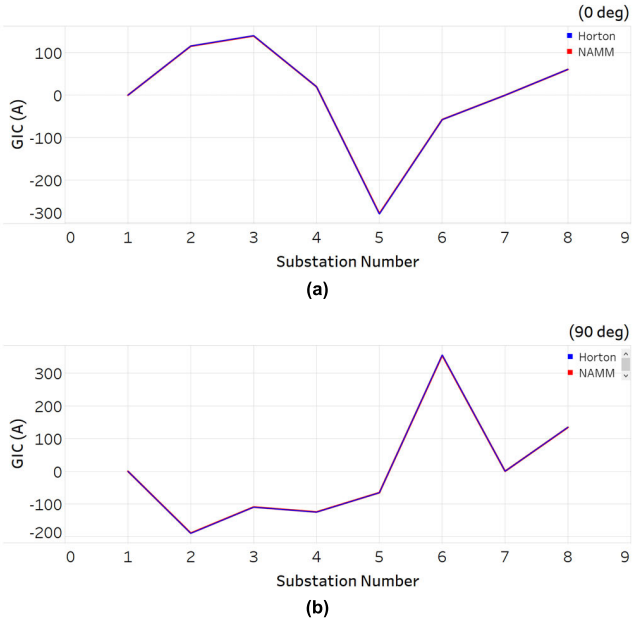

FIGURE 8. GIC values provided in the previous study [49] compared to the values calculated using the NAMM due to the 1 V/km geoelectric field at (a) 0° northward and (b) 90° eastward directions.

B. SIMULATION RESULTS OF CASE 2

This simulation case, the four types of HV power transformers available in the Malaysian power network were operated under the GIC condition and the AC reaction of the system was investigated without connection of the GIC mitigation devices. This analysis was carried out in the PSCAD/EMTDC software using the system model illustrated in Fig. 3, and the transformers' details are presented in Table 2. The controlled voltage sources were used to inject the GICs into the power system through the grounded neutral of the HV sides of transformers. Most of the previous studies have used current sources to represent the GIC flow into the system. This approach is practical when studying the GIC effects on the transformers. However, it is unsuitable in the case modelling GIC mitigation system as the current source model would attempt to force its current through an alternative path when breaking an existing GIC path in the power network. For instance, the GIC might be forced to flow through an open breaker that is purposely modelled as a very large impedance in a mitigation system, producing spurious voltages in the simulation [53]. The waveforms of injected GICs are presented in Fig. 9.

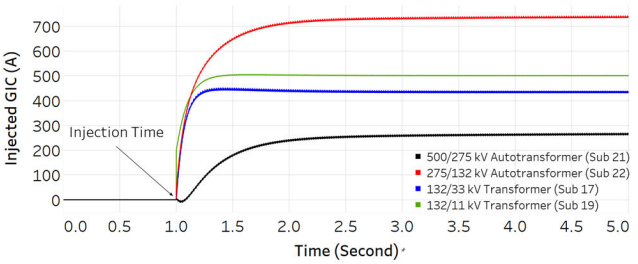

FIGURE 9. GIC waveforms due to 20 V/km geoelectric field at angle 100° injected into neutrals of transformers.

The injected GIC values and locations of transformers were selected based on the results of the previous simulation case due to the geoelectric field of 20 V/km at 100° angle (Fig. 7 (b)). The injection time for all transformers was set to 1 second, assuming that the GMD event starts when the system is under the steady-state condition and the duration time was set to 5seconds. The GIC is divided equally between the phases of star windings transformers. In autotransformers, the GIC flow is divided in all terminals since the series and common windings are linked physically.

When the power transformers are subjected to GICs, DC flux is impressed in the transformer cores, and half-cycle saturation will take place. The magnitude of this DC flux is dependent on the magnitude of the DC current, the number of turns in the windings carrying this current, and the reluctance DC path. During half of the 50-Hz cycle, the DC flux adds to the AC flux and subtracts from the AC flux during the other half cycle, consequently shifting the operating point of the transformer's magnetizing characteristics [54].

After the GICs were injected into the transformers in the Malaysian power model, the half-cycle saturation occurred in the transformers' cores, as depicted in Fig. 10. Based on the figure, the saturation period during the GIC in autotransformers was much longer than other transformers. In other words, the required time to accumulate flux and for the magnetizing current to increase to steady-state was longer for the autotransformers. This was due to the connected tertiary delta winding in the autotransformer acts as damping winding for the DC excitation and works against the DC current in the primary winding. As a result, the increase of DC flux will slow down. Eventually, the flux will finally increase to a similar level as with no tertiary delta winding [55].

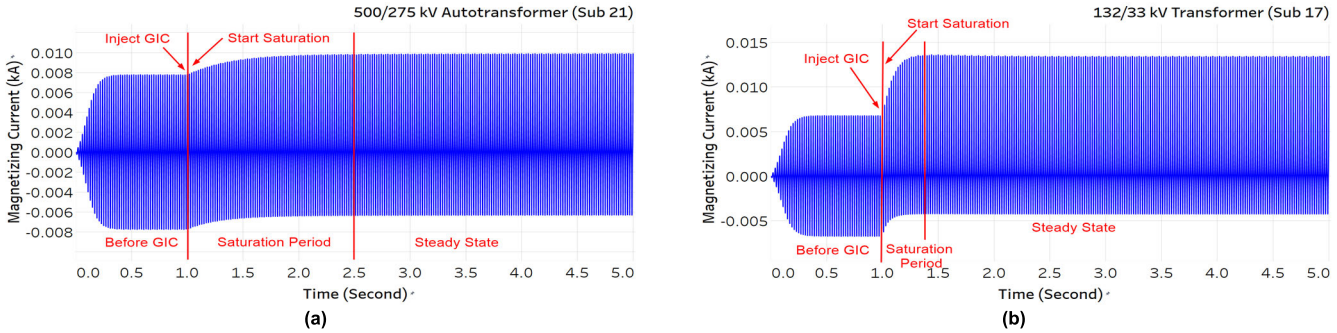

FIGURE 10. Magnetizing currents of transformers before and after GIC (a) 500/275 kV autotransformer at substation 21 (b) 132/33 kV transformer at substation 17.

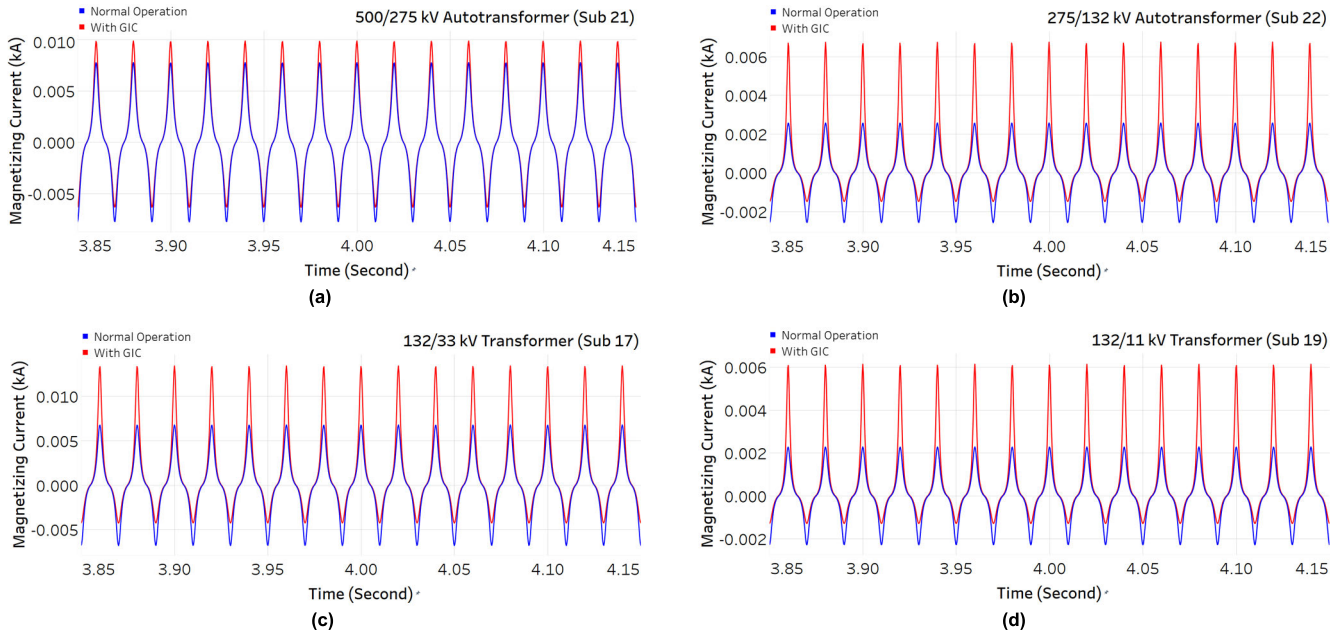

FIGURE 11. Magnetizing currents of different transformers' types in the Malaysian power network under normal operating condition and during GICs in (a) substation 21, (b) substation 22, (c) substation 17, and (d) substation 19.

The simulation results of the magnetizing current, hysteresis, instantaneous current and voltage, and reactive power of transformers with and without GICs are presented in Figs. 11–14. The results of normal operation conditions (no GIC) and with GICs are depicted as blue and red lines, respectively.

As shown in Fig. 11(a), the magnetizing current of the 500/275 kV autotransformer at substation 21 was symmetrical around zero under the normal operating condition with a peak value of 0.0077 kA. When 268 A GIC was injected into this transformer at 1 second simulation time, the magnetizing current was steadily drifted to the positive side. After 1.5 seconds, the half-cycle saturation occurred, and the peak current became 0.0098 kA. In Fig. 11(b), the magnetizing current of 275/132 kV autotransformer at substation 22 without GIC was 0.0025 kA. The magnetizing current was then increased to 0.0067 kA on the positive side when 743 A of GIC was injected into the transformer. Regarding the 132 kV transformers in the system under GIC condition, Fig. 11(c) shows that the magnetizing current of the 132/33 kV transformer at substation 17 was equal to 0.0068 kA under normal operating condition. After 433 A of GIC was injected into the primary winding, the magnetizing current was increased in the positive side of the waveform to 0.0134 kA. While in substation 19, the magnetizing current of the 132/11 kV transformer was asymmetrically increased from 0.0022 kA under normal condition to 0.006 kA after 505 A of GIC was injected into the primary side (Fig. 11(d)).

In addition, the hysteresis curves of the transformers during normal AC operating condition with and without GIC are presented in Fig. 12 to illustrate the half-cycle phenomena more clearly. As shown in the figure, with no GIC, the curves were symmetrical around the zero-flux point and the peak

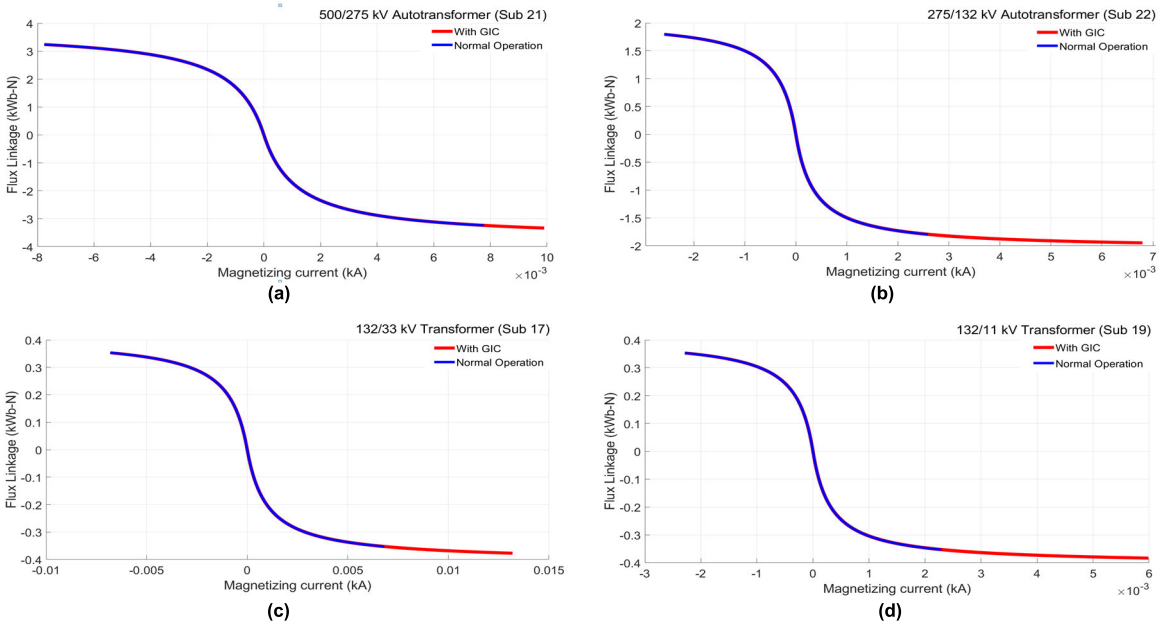

FIGURE 12. Hysteresis curve of different transformers' types in the Malaysian power network under normal operating condition and during GICs.

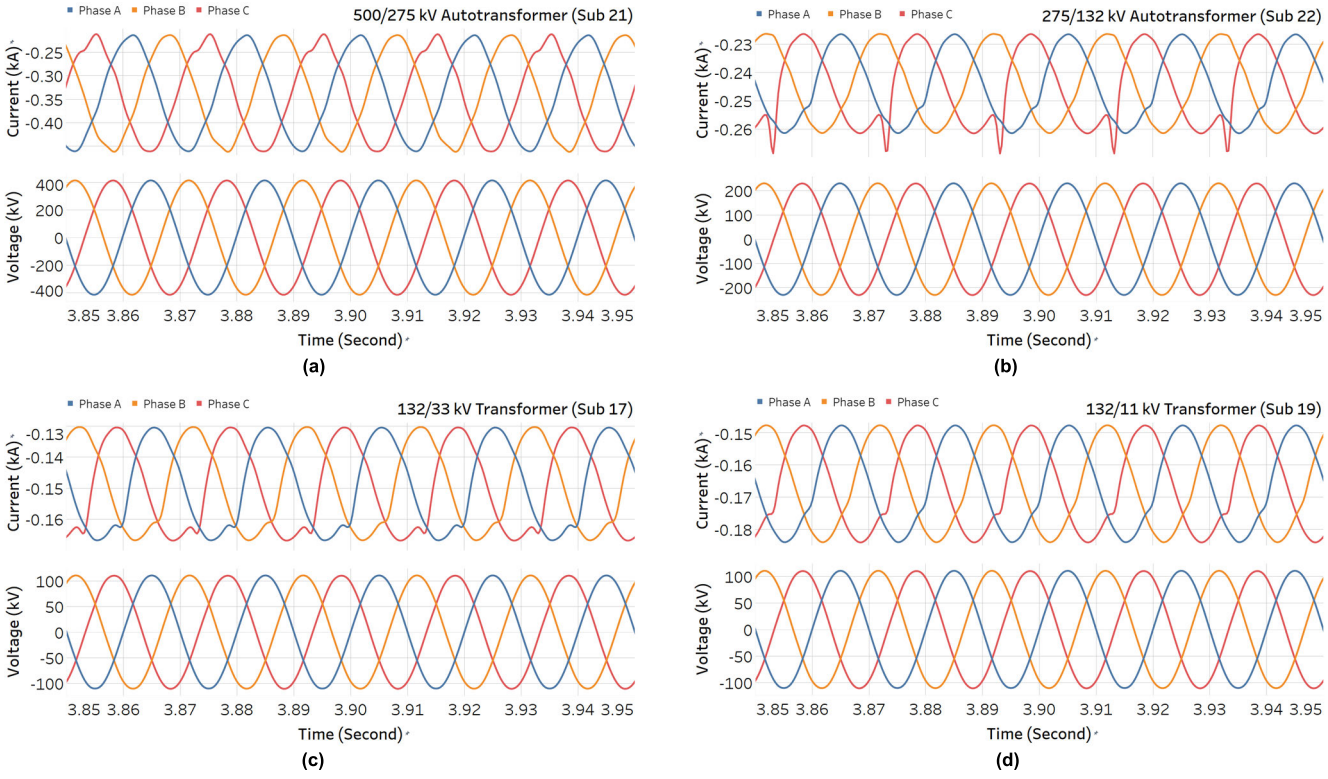

FIGURE 13. Current and voltage waveforms at the primary sides of different transformers' types in the Malaysian power network during GICs.

AC fluxes lay just under the knee points of the nonlinear characteristics. When the DC fluxes were added to the AC fluxes under a GIC condition, the transformers' cores were driven into the saturation region with asymmetric fluxes that exceeded the knee point in one of the half-cycles, as depicted in red lines. It is because a slight increase of the flux requires a very large increase of the magnetization current. Consequently, the amplitude of the magnetization current becomes

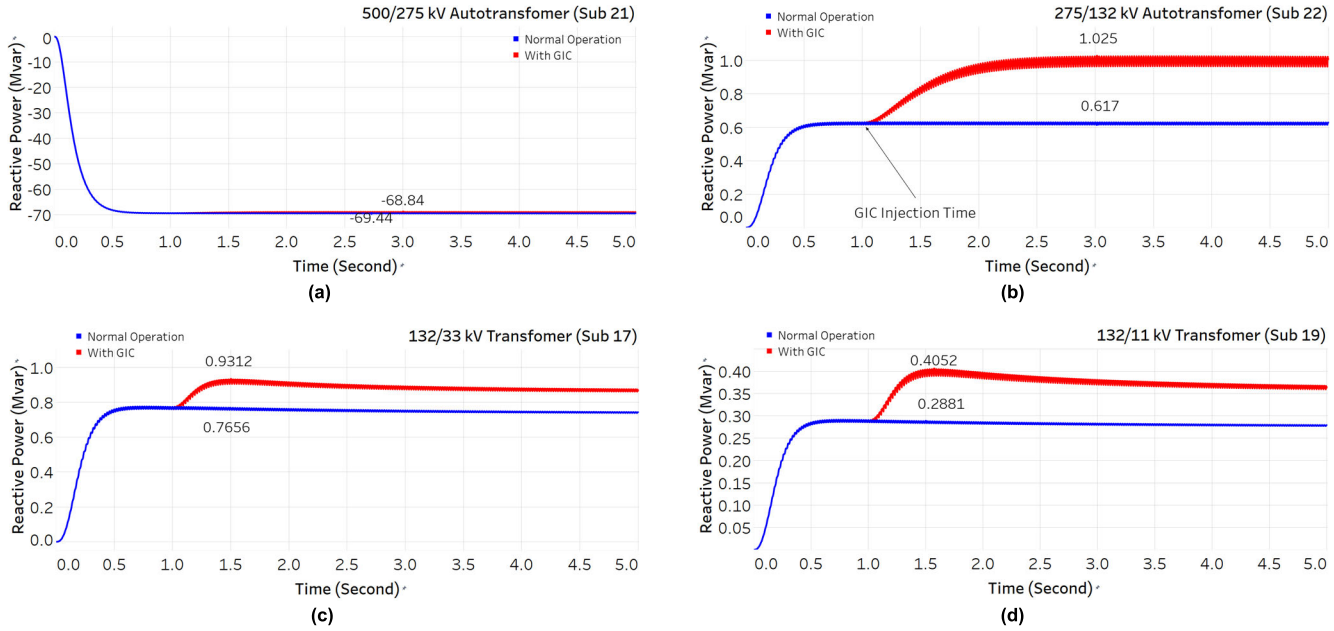

FIGURE 14. Active power of different transformers' types in the Malaysian power network under normal operating and during GICs.

very high in a one-half cycle and decreases slightly in the other half-cycle [56].

The worst saturation occurred in the 275/132 kV and 132/11 kV transformers, as presented in Fig. 12(b) and (d). When the transformer core becomes saturated, the flux leaks and travels outside the core through adjacent paths and is no longer contained within the transformer core. This results in additional flux linkages clamping the structural parts such as tie plates, yoke clamps, tank cover, tank walls, and tank bottom [57]. Similar results were observed in other studies on the magnetizing current [58]. The hotspots may occur in the transformers due to this flux and cause severe damage to the insulation paper of the winding, produce gassing and combustion of the transformer oil or lead to major transformer failures [57], [59].

The impact of the saturation phenomenon could lead to several consequences, such as harmonics in the excitation and secondary currents, an increase reactive power consumption, and a possible transformer breakdown [59]. Based on Fig. 13, the three-phase excitation currents of the transformers at the primary sides drifted to the negative side of the waveforms and were accompanied by high harmonic distortions under GIC conditions. These distortions reflect the sensitivity of the transformers to DC excitation during GMD events [55]. In Fig.13(a), the peak-to-peak excitation current in the 500/275 kV autotransformer was in the range of −0.21 to −0.46 kA. While in the 275/132 kV autotransformer, the peak-to-peak of excitation current was in the range of −0.22 to −0.26 kA (Fig. 13(b)). Regarding the transformers at substations 17 and 19, the peak-to-peak excitation currents were in the range of −0.13 to −0.16 kA

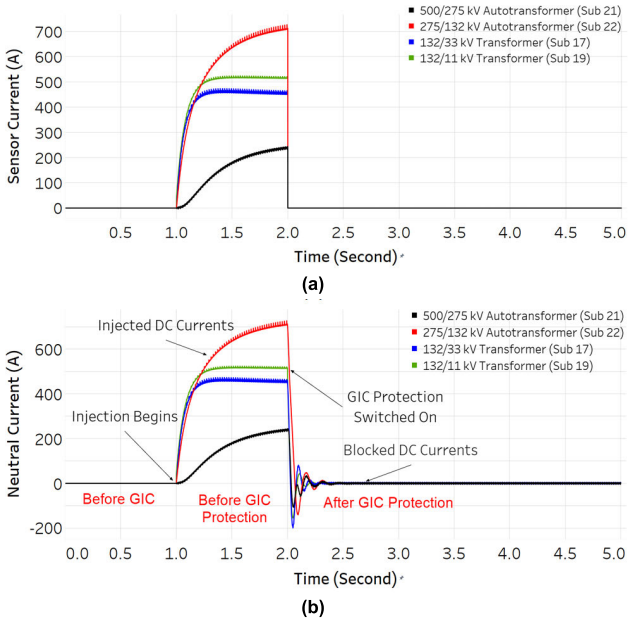

FIGURE 15. Simulation results of (a) sensor currents and (b) neutral currents of transformers during GIC event.

and −0.14 to −0.18 kA in the 132/33 kV and 132/11 kV transformers, respectively, as presented in Fig.13(c) and (d).

In terms of the saturation impacts on the transformers' reactive powers, Fig. 14 shows that the reactive power losses increased during the GICs condition. Because, during GICs, the transformers will turn to an inductive load and consume more reactive power resulting in fluctuations in the voltage

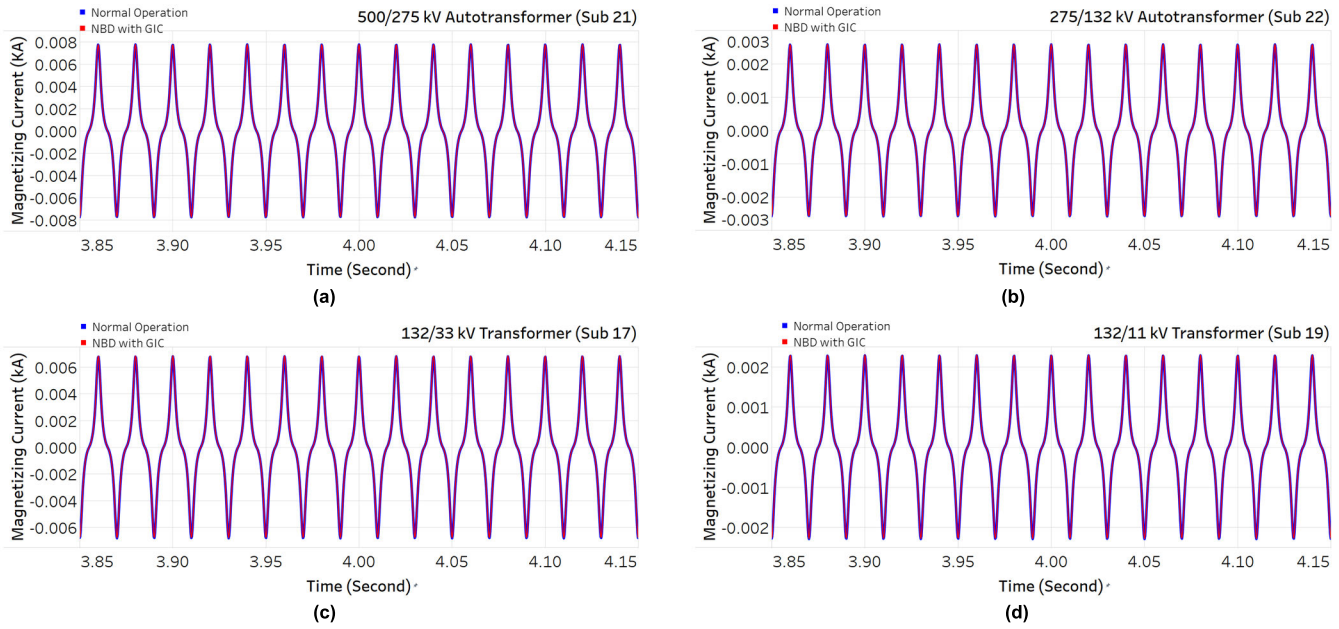

FIGURE 16. Magnetizing current of different transformers' types in the Malaysian power network under normal operating condition and during NBDs operation in (a) substation 21, (b) substation 22, (c) substation 17, and (d) substation 19.

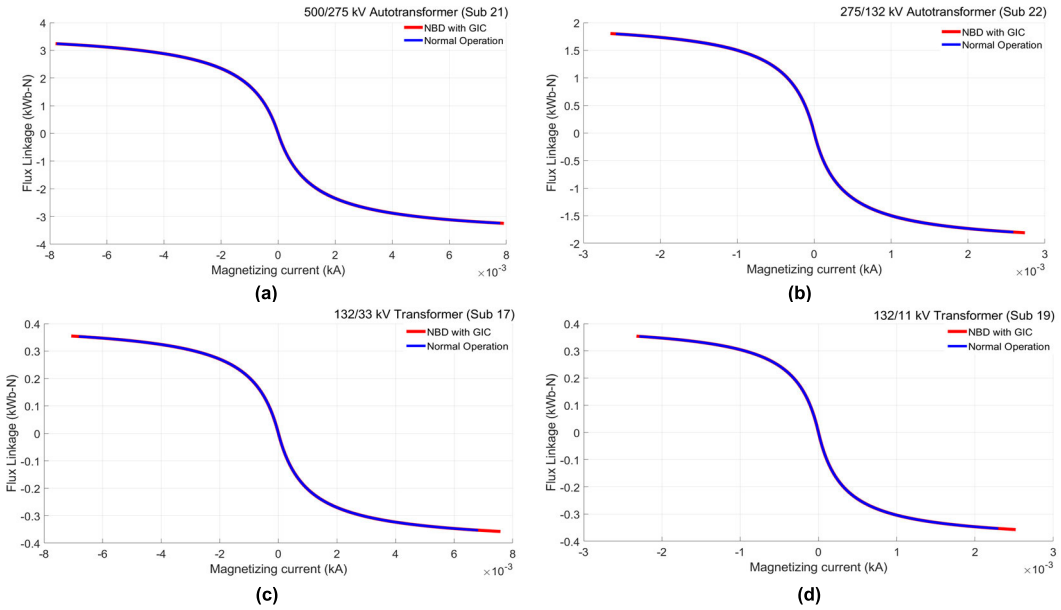

FIGURE 17. Hysteresis curve of different transformers' types in the Malaysian power network under normal operating condition and during NBDs operation.

level. In addition, the reactive power increases to fulfil the magnetization characteristics reported in the previous literature [60]–[63]. The reactive power consumptions of the transformer under the normal exciting current and with GIC condition are calculated based on equations 4 and 5.

$$Q = 3U_1 \cdot I_1 \tag{4}$$

where U_1 and I_1 are the voltage and fundamental harmonic values of the magnetization current in each phase, respectively.

$$Q_{GIC} = k \cdot I_{eff} + Q \tag{5}$$

where k is the Mvar/ampere scaling factor, which depends on the transformer's core type [64], [65] and I_{eff} is the effective value of the GICs flowing in the transformer windings, which is dependent on the transformer's winding type [39].

Fig. 14(b) shows that the reactive power consumption of the 275/132 kV autotransformer has increased from

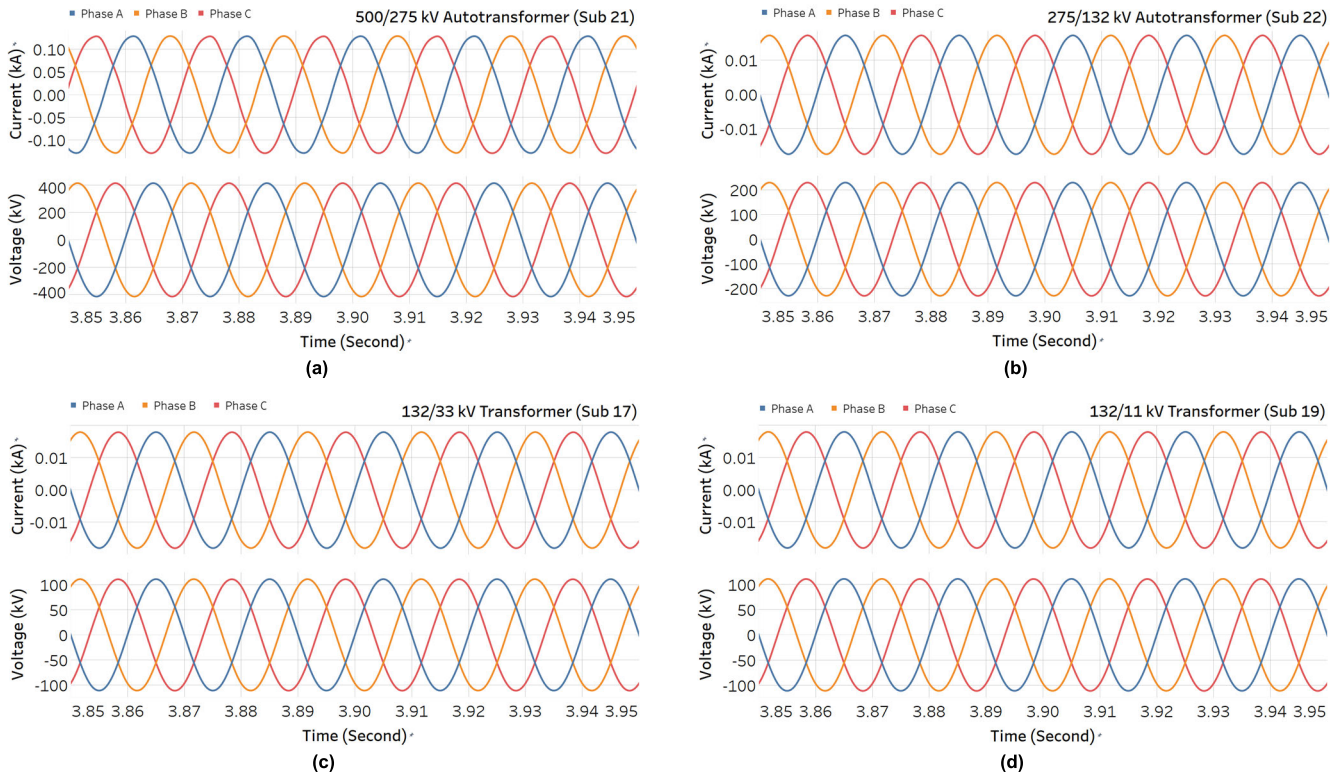

FIGURE 18. Current and voltage waveforms at primary sides of different transformers' types in the Malaysian power network during NBDs operation.

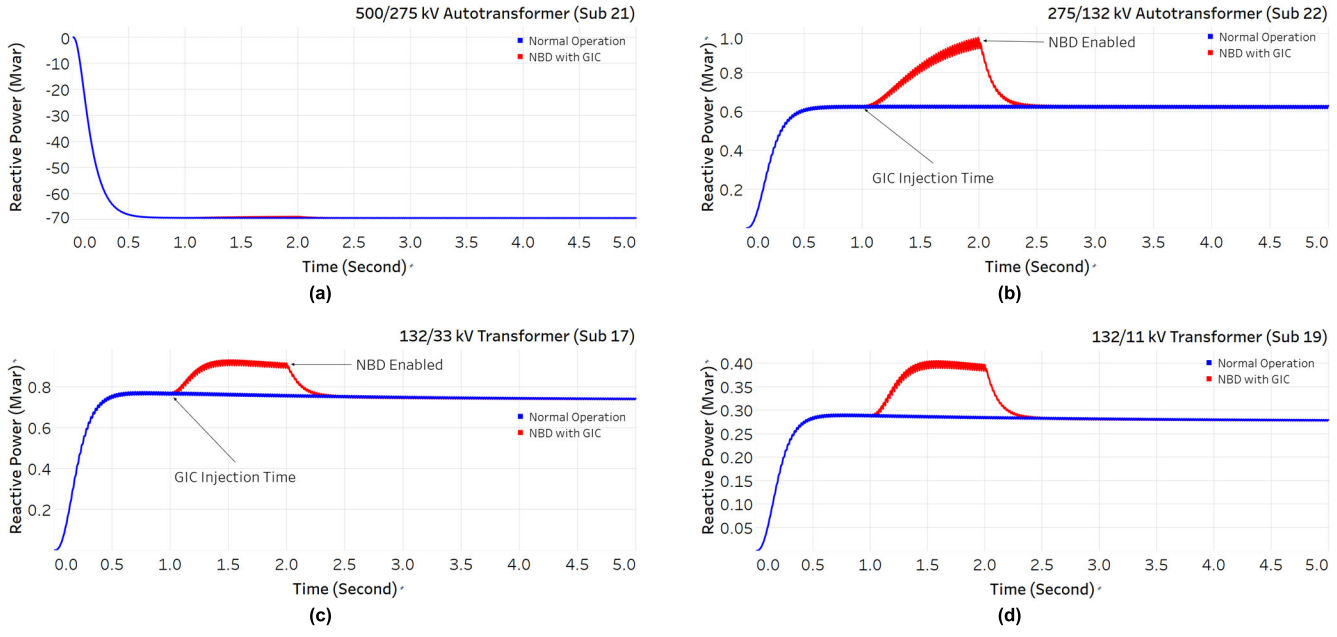

FIGURE 19. Reactive power at primary sides of different transformers' types in the Malaysian power network under normal operating condition and during NBDs operation.

0.61 Mvar to 1.02 Mvar (increased 65.6%) after GIC injection. In substation 17, the reactive power of the 132/33 kV transformer increased from 0.76 Mvar to 0.93 Mvar (increased 22.4%) (Fig. 14(c)). In the 132/11 kV transformer in substation 19, the reactive power increased from 0.28 Mvar to 0.40 Mvar (increased 42.9%) (Fig. 14(d)). Likewise, in the 500/275 kV autotransformer at substation 21, reactive power varied from -69.44 Mvar to -68.84 Mvar (decreased 0.9%), which was considered a slight difference compared to the actual value (Fig. 14(a)). The severity of the saturation and

DC magnetization is dependent on the magnitude of GIC and type of transformer. Usually, single-phase transformers are more vulnerable with respect to this phenomenon compared to the three-phase transformers [56]. Additionally, the size and type of connected loads can influence the severity of the saturation. This test is significant because it establishes some of the principle behaviour patterns of large power transformers during the presence of the GIC intended in-situ environment of the power grid rather than tests in the laboratory environment.

C. SIMULATION RESULTS OF CASE 3

In the third simulation case, the modelled conventional GIC NBD systems in PSCAD were connected to transformers in the same locations of the second simulation case to investigate the efficacy of these systems under such large GIC threat scenarios and during system operation. The same GICs presented in Table 2 and Fig. 9 were injected into the system and the second simulation case was repeated. The GICs injection time was set at 1 second, and the time delay of mitigation systems was set to 2 seconds so that after 1 second of the GMD occurrence, these systems were enabled, as illustrated in Fig. 15(a) and (b).

As shown in Fig. 15, when GICs were detected by sensors of NBD mitigation systems, the solid ground mode switches were opened at 2 seconds, enabling the GIC protection modes, introducing a high impedance to the paths of very low-frequency DC currents and effectively eliminating them. The blocked DC currents were almost equal to zero in the neutral paths of the transformers, where the mitigation systems have been installed. It is more revealing and valuable to do a preliminary evaluation of proposed mitigation strategies using GICs obtained in the Malaysian power network due to the applied geoelectric field of 20 V/km.

Figs. 16–19 present the comparison of magnetizing current, hysteresis, instantaneous current and voltage, and reactive power of transformers under normal operating condition (no GIC) and NBDs operation during the GIC depicted as blue and red lines, respectively. In Fig. 16, it can be seen that the operations of the mitigation devices prevented the saturation of transformers, and their magnetizing currents were symmetrical around zero, which matched with the results under normal operating condition with no GIC so that they overlapped.

Likewise, the hysteresis curves of transformers were centred around zero and laid just under the knee point, which agreed with the results under normal condition (Fig. 17). Also, the obtained simulation results of current and voltage profiles of power transformers at the primary sides after GIC mitigation systems operation were pure (clean) three-phase sinewaves that did not contain harmonic distortions and were symmetrical around zero, as presented in Fig. 18.

Regarding the reactive power outputs of the transformers, Fig. 19 shows that when the installed NBD mitigation systems were switched on after 2 seconds, reactive power losses occurred in the transformers due to the injected induced currents were successfully eliminated. As shown in the figure, during the operation of the GIC mitigation systems, the reactive powers were stabilized at the exact values obtained under normal operating condition with no GIC. Note that the time delay of the mitigation systems was set to 2 seconds to present the differences and display how these systems eliminate the saturation in the transformers. The NBDs installation left no path for the passage of GICs and completely desensitized the network to the impacts of GMD. Moreover, these NBD mitigation systems are also able to provide protection against enhanced GIC due to the detonation of HEMP [10], [66].

IV. CONCLUSION

In this work, the Malaysian power network for GIC impact analysis performance has been implemented using PSCAD/EMTDC software based on the actual data provided by the local power utility. The distribution of GICs in the network due to a geoelectric field of 20 V/km in the northward and eastward directions was investigated and the most susceptible locations to GMD event in the Malaysian power network were estimated. The analysis showed that an electric field pointing at a 100° angle induced the maximum GICs in the whole network. Also, it demonstrated that substations located in the middle of the network and linked to the longer length of transmission lines were the most vulnerable to GMD events and experienced the most severe GIC impacts. The maximum value of GIC was observed at substation 22 with a value of 743A.

Then GIC impacts and saturation levels of four transformer's types in the related locations were investigated over transmission networks. The transformers selected from substations 17, 19, 21, and 22 experienced the highest GICs. The injected GICs caused half-cycle saturation and increased the reactive power consumption of the transformers. Subsequently, the proposed GIC mitigation systems based on NBDs were connected to block the GIC flow in their neutral paths and eliminate its effects. Thus, the results showed that connected NBDs successfully blocked the injected GICs in the neutral ground of transformers and were able to prevent the saturation occurrence. The analysis results provide relevant researchers, engineers and utility operators with a better understanding of the GIC effects and select a suitable GIC mitigation system with the most appropriate ratings for respective locations in the case of GMD events.

REFERENCES

[1] M. Wik, R. Pirjola, H. Lundstedt, A. Viljanen, P. Wintoft, and A. Pulkkinen, "Space weather events in July 1982 and October 2003 and the effects of geomagnetically induced currents on Swedish technical systems," *Ann. Geophys.*, vol. 27, no. 4, pp. 1775–1787, 2009.

[2] D. M. Oliveira and C. M. Ngwira, "Geomagnetically induced currents: Principles," *Brazilian J. Phys.*, vol. 47, no. 5, pp. 552–560, Oct. 2017.

[3] C. M. Ngwira, A. Pulkkinen, M. M. Kuznetsova, and A. Glocer, "Modeling extreme 'Carrington-type' space weather events using three-dimensional global MHD simulations," *J. Geophys. Res., Space Phys.*, vol. 119, no. 6, pp. 4456–4474, 2014.

[4] S. K. Vijapurapu, "Contingency analysis of power systems in presence of geomagnetically induced currents," M.S. thesis, Dept. Elect. Comput. Eng., Univ. Kentucky, Lexington, KY, USA, 2013.

[5] D. M. Oliveira, D. Arel, J. Raeder, E. Zesta, C. M. Ngwira, B. A. Carter, E. Yizengaw, A. J. Halford, B. T. Tsurutani, and J. W. Gjerloev, "Geomagnetically induced currents caused by interplanetary shocks with different impact angles and speeds," *Space Weather*, vol. 16, no. 6, pp. 636–647, Jun. 2018.

[6] C. Huang, "Systematical analyses of global ionospheric disturbance current systems caused by multiple processes: Penetration electric fields, solar wind pressure impulses, magnetospheric substorms, and ULF waves," *J. Geophys. Res., Space Phys.*, vol. 125, no. 9, Sep. 2020, Art. no. e2020JA027942.

[7] S. Watari, S. Nakamura, and Y. Ebihara, "Measurement of geomagnetically induced current (GIC) around Tokyo, Japan," *Earth, Planets Space*, vol. 73, no. 1, pp. 1–19, Dec. 2021.

[8] P. Riley, J. A. Linker, J. A. G. Esparza, L. K. Jian, C. T. Russell, and J. G. Luhmann, "Interpreting some properties of CIRs and their associated shocks during the last two solar minima using global MHD simulations," *J. Atmos. Sol.-Terr. Phys.*, vol. 83, pp. 11–21, Jul. 2012.

[9] Y. Zhang, W. Sun, X. S. Feng, C. S. Deehr, C. D. Fry, and M. Dryer, "Statistical analysis of corotating interaction regions and their geoeffectiveness during solar cycle 23," *J. Geophys. Res., Space Phys.*, vol. 113, no. A8, Aug. 2008, Art. no. A08106.

[10] F. R. Faxvog, W. Jensen, G. Fuchs, G. Nordling, D. B. Jackson, B. Groh, N. Ruehl, A. P. Vitols, T. L. Volkmann, M. R. Rooney, and R. Neal, "Power grid protection against geomagnetic disturbances (GMD)," in *Proc. IEEE Electr. Power Energy Conf.*, Halifax, NS, Canada, Aug. 2013, pp. 1–13.

[11] M. Nazir, K. Burkes, and J. H. R. Enslin, "Converter-based power system protection against DC in transmission and distribution networks," *IEEE Trans. Power Electron.*, vol. 35, no. 7, pp. 6701–6704, Jul. 2020.

[12] S. P. Blake, P. T. Gallagher, J. McCauley, A. G. Jones, C. Hogg, J. Campanyà, C. D. Beggan, A. W. P. Thomson, G. S. Kelly, and D. Bell, "Geomagnetically induced currents in the Irish power network during geomagnetic storms," *Space Weather*, vol. 14, no. 12, pp. 1136–1154, Dec. 2016.

[13] J. Ramírez-Niño, C. Haro-Hernández, J. H. Rodriguez-Rodriguez, and R. Mijarez, "Core saturation effects of geomagnetic induced currents in power transformers," *J. Appl. Res. Technol.*, vol. 14, no. 2, pp. 87–92, Apr. 2016.

[14] R. Pirjola and D. Boteler, "Geomagnetically induced currents in European high-voltage power systems," in *Proc. Can. Conf. Electr. Comput. Eng.*, Ottawa, ON, Canada, 2006, pp. 1263–1266.

[15] M. Heindl, M. Beltle, M. Reuter, D. Schneider, S. Tenbohlen, D. T. Oyedokun, and C. T. Gaunt, "Investigation of GIC related effects on power transformers using modern diagnostic methods," in *Proc. Int. Symp. High Voltage Eng.*, Hannover, Germany, 2011, pp. 1–6.

[16] R. Zhang, "Transformer modelling and influential parameters identification for geomagnetic disturbances events," Ph.D. dissertation, Dept. Elect. Electron. Eng., Univ. Manchester, Manchester, U.K., 2012.

[17] A. A. Hussein and M. H. Ali, "Suppression of geomagnetic induced current using controlled ground resistance of transformer," *Electr. Power Syst. Res.*, vol. 140, pp. 9–19, Nov. 2016.

[18] R. Caraballo, "Geomagnetically induced currents in uruguay: Sensitivity to modelling parameters," *Adv. Space Res.*, vol. 58, no. 10, pp. 2067–2075, Nov. 2016.

[19] R. L. Bailey, T. S. Halbedl, I. Schattauer, A. Römer, G. Achleitner, C. D. Beggan, V. Wesztergom, R. Egli, and R. Leonhardt, "Modelling geomagnetically induced currents in midlatitude central Europe using a thin-sheet approach," in *Annales Geophysicae*, vol. 35, no. 3. Munich, Germany: European Geosciences Union, 2017, pp. 751–761.

[20] N. Chiesa, A. Lotfi, H. K. Høidalen, B. Mork, Ø. Rui, and T. Ohnstad, "Five-leg transformer model for GIC studies," in *Proc. Int. Conf. Power Syst. Transients (IPST)*, Vancouver, BC, Canada, 2013, pp. 1–6.

[21] F. Aboura and O. Touhami, "Effect of the GICs on magnetic saturation of asymmetric three-phase transformer," *IET Electr. Power Appl.*, vol. 11, no. 7, pp. 1306–1314, Aug. 2017.

[22] C.-M. Liu, L.-G. Liu, and R. Pirjola, "Geomagnetically induced currents in the high-voltage power grid in China," *IEEE Trans. Power Del.*, vol. 24, no. 4, pp. 2368–2374, Oct. 2009.

[23] A. Foss and D. Boteler, "GIC simulation using network modeling," in *Proc. IEEE Can. Conf. Elect. Comput. Eng. (CCECE)*, Ottawa, ON, Canada, 2006, pp. 1–4.

[24] R. P. Jayasinghe, "Investigation of protection problems due to geomagnetically induced currents," Ph.D. dissertation, Dept. Elect. Comput. Eng., Univ. Manitoba, Winnipeg, MB, Canada, 1996.

[25] Z. M. K. Abda, N. F. A. Aziz, M. Z. A. A. Kadir, and Z. A. Rhazali, "A review of geomagnetically induced current effects on electrical power system: Principles and theory," *IEEE Access*, vol. 8, pp. 200237–200258, 2020.

[26] E. B. Seba and M. Nigussie, "Investigating the effect of geomagnetic storm and equatorial electrojet on equatorial ionospheric irregularity over East African sector," *Adv. Space Res.*, vol. 58, no. 9, pp. 1708–1719, Nov. 2016.

[27] V. Doumbia, K. Boka, N. Kouassi, O. D. F. Grodji, C. Amory-Mazaudier, and M. Menvielle, "Induction effects of geomagnetic disturbances in the geo-electric field variations at low latitudes," in *Annales Geophysicae*, vol. 35, no. 1. Göttingen, Germany: Copernicus GmbH, 2017, pp. 39–51.

[28] K. G. Simi, G. Manju, M. K. M. Haridas, S. R. P. Nayar, T. K. Pant, and S. Alex, "Ionospheric response to a geomagnetic storm during November 8–10, 2004," *Earth, Planets Space*, vol. 65, no. 4, pp. 343–350, Apr. 2013.

[29] R. G. Rastogi, "Magnetic storm effects at equatorial electrojet stations," *Earth, Planets Space*, vol. 58, no. 5, pp. 645–657, May 2006.

[30] E. Astafyeva, I. Zakharenkova, K. Hozumi, P. Alken, P. Coïsson, M. R. Hairston, and W. R. Coley, "Study of the equatorial and low-latitude electrodynamic and ionospheric disturbances during the 22–23 June 2015 geomagnetic storm using ground-based and spaceborne techniques," *J. Geophys. Res., Space Phys.*, vol. 123, no. 3, pp. 2424–2440, Mar. 2018.

[31] K. K. Hashimoto, T. Kikuchi, I. Tomizawa, K. Hosokawa, J. Chum, D. Buresova, M. Nose, and K. Koga, "Penetration electric fields observed at middle and low latitudes during the 22 June 2015 geomagnetic storm," *Earth, Planets Space*, vol. 72, no. 1, pp. 1–15, Dec. 2020.

[32] Z. I. A. Latiff, M. H. Jusoh, and K. Burhanudin, "Assessment of geomagnetically induced currents in low latitude regions with respect to severe geomagnetic storm over solar cycle 24," in *J. Phys., Conf. Ser.*, vol. 1768, no. 1, Jan. 2021, Art. no. 012002.

[33] O. Anaya-Lara and E. Acha, "Modeling and analysis of custom power systems by PSCAD/EMTDC," *IEEE Trans. Power Del.*, vol. 17, no. 1, pp. 266–272, Jan. 2002.

[34] PSCAD, Manitoba Hydro International. *PSCAD Professional/Commercial, Educational, Trial, and Free Editions*. Accessed: Oct. 27, 2021. [Online]. Available: https://www.pscad.com/knowledge-base/article/52

[35] H. Saadat, *Power System Analysis*. New York, NY, USA: McGraw-Hill, 1999.

[36] A. J. McKay, "Geoelectric fields and geomagnetically induced currents in the United Kingdom," Ph.D. dissertation, Dept. Geol. Geophys., Univ. Edinburgh, Edinburgh, U.K., 2004.

[37] M. F. Faisal, *Voltage Sag Solutions for Industrial Customers (A Guidebook by Tenaga Nasional Berhad)*. Kuala Lumpur, Malaysia: Tenaga Nasional Berhad, 2018.

[38] A. Pulkkinen, E. Bernabeu, J. Eichner, C. Beggan, and A. W. P. Thomson, "Generation of 100-year geomagnetically induced current scenarios," *Space Weather*, vol. 10, no. 4, 2012, Art. no. S04003.

[39] K. Patil, "Modeling and evaluation of geomagnetic storms in the electric power system," in *Proc. Int. Council Large Electr. Syst. (CIGRE)*, New York, NY, USA, 2014, pp. 1–8.

[40] A. D. Rajapakse, N. Perera, F. R. Faxvog, W. Jensen, G. Nordling, G. Fuchs, D. B. Jackson, T. L. Volkmann, N. Ruehl, and B. Groh, "Power grid stability protection against GIC using a capacitive grounding circuit," in *Proc. PES T&D*, Orlando, FL, USA, May 2012, pp. 1–6.

[41] K. Mukhtar, M. Ingham, C. J. Rodger, D. H. M. Manus, T. Divett, W. Heise, E. Bertrand, M. Dalzell, and T. Petersen, "Calculation of GIC in the north island of New Zealand using MT data and thin-sheet modeling," *Space Weather*, vol. 18, no. 11, Nov. 2020, Art. no. e2020SW002580.

[42] E. Arajärvi, R. Pirjola, and A. Viljanen, "Effects of neutral point reactors and series capacitors on geomagnetically induced currents in a high-voltage electric power transmission system," *Space Weather*, vol. 9, no. 11, pp. 1–10, 2011.

[43] R. L. Bailey, T. S. Halbedl, I. Schattauer, G. Achleitner, and R. Leonhardt, "Validating GIC models with measurements in austria: Evaluation of accuracy and sensitivity to input parameters," *Space Weather*, vol. 16, no. 7, pp. 887–902, Jul. 2018.

[44] R. Caraballo, J. A. González-Esparza, M. Sergeeva, and C. R. Pacheco, "First GIC estimates for the Mexican power grid," *Space Weather*, vol. 18, no. 2, Feb. 2020, Art. no. e2019SW002260.

[45] S. Blake, "Modelling and monitoring geomagnetically induced currents in Ireland," Ph.D. dissertation, School Phys., Trinity College Dublin, Dublin, Ireland, 2017.

[46] B.-S. Joo, J.-W. Woo, J.-H. Lee, I. Jeong, J. Ha, S.-H. Lee, and S. Kim, "Assessment of the impact of geomagnetic disturbances on Korean electric power systems," *Energies*, vol. 11, no. 7, p. 1920, Jul. 2018.
[47] C. D. F. Barroso, "GIC distribution," Lund Univ., Lund, Sweden, Tech. Rep., 2014.
[48] M. Myllys, A. Viljanen, Ø. A. Rui, and T. M. Ohnstad, "Geomagnetically induced currents in Norway: The northernmost high-voltage power grid in the world," *J. Space Weather Space Climate*, vol. 4, p. A10, Mar. 2014.
[49] R. Horton, D. Boteler, T. J. Overbye, R. Pirjola, and R. C. Dugan, "A test case for the calculation of geomagnetically induced currents," *IEEE Trans. Power Del.*, vol. 27, no. 4, pp. 2368–2373, Oct. 2012.
[50] S.-M. Zhang and L.-G. Liu, "A mitigation method based on the principle of GIC-even distribution in whole power grids," *IEEE Access*, vol. 8, pp. 65096–65103, 2020.
[51] G. S. Kelly, A. Viljanen, C. D. Beggan, and A. W. P. Thomson, "Understanding GIC in the UK and French high-voltage transmission systems during severe magnetic storms," *Space Weather*, vol. 15, no. 1, pp. 99–114, Jan. 2017.
[52] A. H. Etemadi and A. Rezaei-Zare, "Optimal placement of GIC blocking devices for geomagnetic disturbance mitigation," *IEEE Trans. Power Syst.*, vol. 29, no. 6, pp. 2753–2762, Mar. 2014.
[53] A. D. Rajapakse and N. Perera, "Simulation of transformer GIC mitigation using neutral DC current and voltage harmonic level to switch in a capacitor to the grounding circuit," Emprimus LLC, Final Rep., 2011.
[54] *Effects of Geomagnetic Disturbances on the Bulk Power System*, North Amer. Electr. Rel. Corp., Atlanta, GA, USA, 2012.
[55] J. Xie, "Time domain analysis of the impact of geomagnetically induced current on power system," Ph.D. dissertation, School Elect. Comput. Eng., Georgia Inst. Technol., Atlanta, GA, USA, 2020.
[56] S. A. Mousavi and D. Bonmann, "Analysis of asymmetric magnetization current and reactive power demand of power transformers due to GIC," *Proc. Eng.*, vol. 202, pp. 264–272, 2017.
[57] R. Girgis and K. Vedante, "Effects of GIC on power transformers and power systems," in *Proc. IEEE PES Transmiss. Distrib. (PES T&D)*, Orlando, FL, USA, May 2012, pp. 1–8.
[58] J. E. Berge, "Impact of geomagnetically induced currents on power transformers," Ph.D. dissertation, Dept. Elect. Comput. Eng., Univ. Western Ontario, London, ON, Canada, 2011.
[59] A. A. Zawawi, N. Aziz, M. Z. A. A. Kadir, H. Hashim, and Z. Mohammed, "Evaluation of geomagnetic induced current on 275 kV power transformer for a reliable and sustainable power system operation in Malaysia," *Sustainability*, vol. 12, no. 21, p. 9225, 2020.
[60] H. K. Chisepo, "The response of transformers to geomagnetically induced-like currents," M.S. thesis, Dept. Elect. Eng., Univ. Cape Town, Cape Town, South Africa, 2014.
[61] T. S. Molinski, "Why utilities respect geomagnetically induced currents," *J. Atmos. Sol.-Terr. Phys.*, vol. 64, no. 16, pp. 1765–1778, Nov. 2002.
[62] L. Marti, J. Berge, and R. K. Varma, "Determination of geomagnetically induced current flow in a transformer from reactive power absorption," *IEEE Trans. Power Del.*, vol. 28, no. 3, pp. 1280–1288, Jul. 2013.
[63] J. Berge, R. K. Varma, and L. Marti, "Laboratory validation of the relationship between geomagnetically induced current (GIC) and transformer absorbed reactive power," in *Proc. IEEE Electr. Power Energy Conf.*, Oct. 2011, pp. 491–495.
[64] X. Dong, Y. Liu, and J. G. Kappenman, "Comparative analysis of exciting current harmonics and reactive power consumption from GIC saturated transformers," in *Proc. IEEE Power Eng. Soc. Winter Meeting, Conf.*, vol. 1, Feb. 2001, pp. 318–322.
[65] S. Dahman. (2019). Modeling GMD in powerWorld simulator. PowerWorld Corporation. [Online]. Available: https://www.powerworld.com/files/G02_GMD_In_Simulator.pdf
[66] V. Gurevich, "Protecting power equipment against magnetohydrodynamic effects (MHD) of electromagnetic pulses (EMP)," *Serbian J. Electr. Eng.*, vol. 12, no. 3, pp. 321–332, 2015.